Conductances between confined rough walls

Franck Plouraboué, Sandrine Geoffroy, Marc Prat

▶ **To cite this version:**

Franck Plouraboué, Sandrine Geoffroy, Marc Prat. Conductances between confined rough walls. Physics of Fluids, 2004, 16 (3), pp.615-624. 10.1063/1.1644152 . hal-03601855

HAL Id: hal-03601855
https://hal.science/hal-03601855

Submitted on 8 Mar 2022

HAL is a multi-disciplinary open access archive for the deposit and dissemination of scientific research documents, whether they are published or not. The documents may come from teaching and research institutions in France or abroad, or from public or private research centers.

L'archive ouverte pluridisciplinaire **HAL**, est destinée au dépôt et à la diffusion de documents scientifiques de niveau recherche, publiés ou non, émanant des établissements d'enseignement et de recherche français ou étrangers, des laboratoires publics ou privés.

Conductances between confined rough walls

F. Plouraboué, S. Geoffroy, and M. Prat
Institut de Mécanique des Fluides de Toulouse, UMR CNRS-INPT/UPS No. 5502,
Avenue du Professeur Camille Soula, 31400 Toulouse, France

Two- and three-dimensional creeping flows and diffusion transport through constricted and possibly rough surfaces are studied. Asymptotic expansions of conductances are derived as functions of the constriction local geometry. The validity range of the proposed theoretical approximations is explored through a comparison either with available exact results for specific two-dimensional aperture fields or with direct numerical computations for general three-dimensional geometries. The large validity range of the analytical expressions proposed for the hydraulic conductivity (and to a lesser extent for the electrical conductivity) opens up interesting perspectives for the simulation of flows in highly complicated geometries with a large number of constrictions.

I. INTRODUCTION

In this article we analytically determine the conductances of the incompressible, steady, noninertial flow of a Newtonian fluid through a constriction using the lubrication approximation. Such a flow can be found in various systems or processes, such as rough fractures,[1,2] static seals formed by the compression of two rough metallic surfaces,[3] or micro-fluidic systems.[4] Another interesting context involving a similar problem is the Plateau borders fluid film formed at foam lamela crossings. The swelling of these fluid films has a drastic influence on the mechanical behavior of the foam, the geometry of which is directly related to its hydraulic conductance and, thus, to its swelling dynamic. In all these systems, the local slope is small and the variations of the local aperture are slow, so that one can rely on the (Reynolds) lubrication approximation to analyze the flow. For all confined fluid films in two- or three-dimensional geometries pressure gradients are predominant in localized regions. In two dimensions, these regions are naturally located in the vicinity of the aperture minima [see Fig. 1(a)] while in three dimensions constrictions are located in the vicinity of saddle points. Figure 1(b) shows a schematic representation of such a three-dimensional geometry where constrictions, associated with saddle points of the aperture field, are illustrated. When the mean distance between the two surfaces is sufficiently small for the aperture at a saddle point to be significantly smaller than the mean aperture within the two adjacent valleys, it is expected that the hydraulic flow resistance will be mainly controlled by the saddle point region. Such lubricated flow between confined surfaces has already received a considerable amount of attention in the literature.

In two dimensions, the creeping flow between two cylinders is an old lubrication problem that was first considered by Martin[5] and was later reexamined through lubrication theory by Keller.[6] The generalization of this leading order lubrication analysis to any general elliptic cylinder is trivial. Numerous other studies have considered two-dimensional geometries, with[7,8] or without[9–15] inertia effects. Nevertheless, most of these theoretical investigations were interested in the weakly perturbed limit of large constrictions for which the amplitude of variations is small when compared to the mean diameter.[7–9,16,17] On the other hand, some of them bore on the opposite situation of small constrictions, for which the macroscopic behavior of the flow can display singularities, as first shown by Richardson.[10,15,18–21] Hence, in this case, it is interesting to develop analytical solutions that can be useful either to match numerical boundary conditions, or to directly provide a good approximation for the macroscopic hydrodynamical behavior. As emphasized in Refs. 22 and 23, macroscopic singularities strongly depend on the local geometry of the surfaces which are close to contact. If the surface mean slope (defined as the surface average of the aperture gradient) is zero, the leading order singularities will depend on the surface curvature at the minimum gap. But if the curvature is zero at the minimum gap, then the lubrication leading order will be controlled by higher order surface derivatives as first noticed in Ref. 23. This study focuses on the simple situation of constant applied potential (i.e., pressure or electrical potential) for static solid surfaces. This article investigates the correction to the leading order lubrication theory in two dimensions.

In three dimensions, there has also been a considerable amount of literature regarding creeping flow between solid surfaces in different contexts such as sedimentation and suspension. The hydrodynamical interaction between close particles is strongly dominated by lubrication, the result of which is generally singular with the minimum gap distance. Hence, the detailed hydrodynamic of this confined flow is worth being considered analytically to provide useful boundary conditions for numerical methods.[24] An extensive literature reviewed in Ref. 25 has been devoted to the analysis of three-dimensional lubricated flows. To cite only a few, the analysis of the forces and couple acting on a rotating sphere was first investigated by Dean and O'Neil[26] using matched asymptotic expansion technique. The case of a moving sphere with constant velocity near a wall was then solved by

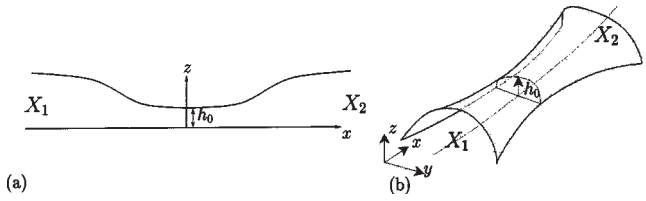

FIG. 1. (a) Schematic representation of a two-dimensional constriction. (b) Schematic representation of a three-dimensional constriction, for which the aperture saddle point is associated with a positive and a negative curvature. Boundary conditions are applied at the aperture field maxima 1 and 2.

O'Neill and Stewartson[27] and Goldman *et al.*[28] The case in which the particle is confined inside a tube has been treated by Bungay and Brenner[29] while other more complex solid surfaces have also been considered.[30,31] The most general case of two oblate spheroids in relative translation was finally addressed by Cox.[32] To the authors' knowledge, however, all these studies have considered two surfaces with positive curvature, for they were mainly addressed in the context of the relative motion of particles. This article focuses on the hydrodynamics of the confined flow between two surfaces with curvatures of opposite sign, as displayed in Fig. 1(b). Nevertheless, such saddle point geometries have already been studied in the context of electro-magnetic transport properties[19–21] (such as equivalent impedance) for which it has been shown that the macroscopic transport parameter depends on the principal curvatures at the saddle. This problem turns out to be different from those previously examined in the lubrication theory context because it brings to the fore a specific geometrical rescaling of longitudinal, transverse and vertical directions.

The purpose of this work is to give an analytical approximation of conductances associated with a constant applied potential (pressure or electrical potential) between two confined surfaces, as well as their validity range in two and three dimensions.

II. GOVERNING EQUATIONS AND DEFINITIONS

A. Governing equation

Let us define the aperture field $\tilde{h}$ as being the local distance between two smoothly spatially varying surfaces.

We will first solve the Poisson problem for the electrical potential $\tilde{\phi}$,

$$\nabla^2\tilde{\phi}=0, \tag{1}$$

with no-flux boundary conditions at the side walls,

$$\partial_n\tilde{\phi}=0 \quad \text{on} \quad \tilde{z}=0 \quad \text{and} \quad \tilde{z}=\tilde{h}, \tag{2}$$

associated with nonconducting boundaries. The local electrical flux density reads $I=D\nabla\tilde{\phi}$ where D is the electrical conductivity. This problem is analogous to the problem of binary diffusion of a species in the dilute limit and heat conduction when the solid walls are of electrical or thermal negligible conductivity. In the context of diffusion (resp. heat conduction) D is the binary diffusion coefficient (resp. the thermal conductivity) and $\tilde{\phi}$ the concentration (resp. the temperature). The results obtained in this article will be presented in the context of electrical conductance. There can nevertheless be directly applied to the thermal conductance problem when it is decoupled from the solid wall.

The electrical conductance G is then related to the electrical flux I and the potential difference $\Delta\tilde{\Phi}=\tilde{\Phi}(X_2)-\tilde{\Phi}(X_1)$ applied at the aperture maxima X_1 and X_2 (see Fig. 1) apart from distance $|X_2-X_1|=L$:

$$I=-DG\frac{\Delta\tilde{\Phi}}{L}. \tag{3}$$

In two dimensions I is the total current per unit width, while in three dimensions the total current is IL. The purpose of the analysis is to look for an asymptotic estimate for this conductance as the aperture at the saddle point becomes small (compared to the apertures of the adjacent valleys).

We will then address the Stokes problem, defined on the pressure $\tilde{p}$ and velocity $\tilde{\mathbf{u}}=(\tilde{u},\tilde{v},\tilde{w})$,

$$-\nabla\tilde{p}+\mu\nabla^2\tilde{\mathbf{u}}=0, \tag{4}$$

where μ is the fluid dynamic viscosity. This momentum equation is complemented by incompressibility:

$$\nabla\cdot\tilde{\mathbf{u}}=0. \tag{5}$$

We apply no slip boundary conditions at the side walls:

$$\tilde{\mathbf{u}}=\mathbf{0} \quad \text{on} \quad \tilde{z}=0, \quad \text{and} \quad \tilde{z}=\tilde{h}. \tag{6}$$

These boundary conditions restrict the presented analysis to nonmobile walls, and excludes the case of surface-driven flows. The hydraulic conductance K is related to the fluid flux Q and the pressure difference $\Delta\tilde{P}=\tilde{P}(X_2)-\tilde{P}(X_1)$ applied at the aperture maxima X_1 and X_2 apart from distance L:

$$Q=-\frac{K}{\mu}\frac{\Delta\tilde{P}}{L}. \tag{7}$$

With this definition, in two dimensions Q is the total flux per unit width, while in three dimensions the total injected flux is QL.

B. Nondimensionalization

In the vicinity of the aperture minimum a Taylor expansion of the two-dimensional aperture field gives

$$\tilde{h}(x)=h_0+\tfrac{1}{2}h_{\tilde{x}\tilde{x}}\tilde{x}^2+\tfrac{1}{6}h_{\tilde{x}\tilde{x}\tilde{x}}\tilde{x}^3+\tfrac{1}{24}h_{\tilde{x}\tilde{x}\tilde{x}\tilde{x}}\tilde{x}^4+\cdots. \tag{8}$$

This expression can be much simplified using the proper nondimentionalization associated with standard lubrication problems.[22] We define ϵ as the ratio of the minimum gap h_0 to its longitudinal curvature $1/h_{\tilde{x}\tilde{x}}$, $\epsilon=\sqrt{h_0h_{\tilde{x}\tilde{x}}}$. This article mainly investigates geometrical situations where $\epsilon<1$. The horizontal direction is then scaled with a slowly varying variable $x=\epsilon\tilde{x}/h_0$ while the vertical direction is simply scaled by the minimum aperture ($z=\tilde{z}/h_0$, $h=\tilde{h}/h_0$). Then, x has been rescaled so that the aperture field in the inner region has, at leading order, a simple parabolic shape,

$$h(x)=1+\tfrac{1}{2}x^2+\epsilon\gamma_3x^3+\epsilon^2\gamma_4x^4+O(\epsilon^3)+\cdots, \tag{9}$$

where we have introduced coefficients $\gamma_3 = h_{\tilde{x}\tilde{x}\tilde{x}}/(6h_{\tilde{x}\tilde{x}}^2)$ and $\gamma_4 = h_{\tilde{x}\tilde{x}\tilde{x}\tilde{x}}/(24h_{\tilde{x}\tilde{x}}^3)$. In the following, we will sometimes use notation $\hat{h}$ for $\hat{h}(x) = 1 + \frac{1}{2}x^2$.

In three dimensions, a Taylor expansion in the vicinity of the aperture saddle point keeping only the first quadratic terms reads

$$\tilde{h}(x,y) = h_0 + \tfrac{1}{2}h_{\tilde{x}\tilde{x}}\tilde{x}^2 + \tfrac{1}{2}h_{\tilde{y}\tilde{y}}\tilde{y}^2 + \cdots, \tag{10}$$

where $h_{\tilde{x}\tilde{x}} > 0$ and $h_{\tilde{y}\tilde{y}} < 0$. The simple nondimensionalization choice for $\tilde{y}$ in the case of two solid convex surfaces with positive curvature should have been identical to the one used in the x direction (see, for example Ref. 32). This simple choice should also correspond to nondimensionalizing using the gap span $\ell = \sqrt{h_0/h_{\tilde{y}\tilde{y}}}$. Nevertheless, a more careful inspection of the specificity of the geometry depicted on Fig. 1(b) rather suggests another choice, because the flow is restricted in the transverse y direction by boundary conditions. Lubrication involves the ratio between the surface curvature and the typical small length-scale in the y direction which is the half-width ℓ. Hence there is a new intrisic small parameter in the problem based on the ratio between the gap span and the transverse curvature $\sqrt{\ell h_{\tilde{y}\tilde{y}}}$ which scales as $\sim\sqrt{\epsilon}$. Then, rescaling $y = \sqrt{\epsilon}\tilde{y}/h_0$, the three-dimensional aperture field is simplified into

$$h(x,y) = 1 + \tfrac{1}{2}x^2 + \epsilon(\tfrac{1}{2}\gamma_2 y^2 + \gamma_3 x^3) + O(\epsilon^{3/2}), \tag{11}$$

where we have introduced coefficient $\gamma_2 = h_{yy}/h_{xx} < 0$ which is $O(1)$. The potential and pressure are nondimensionalized using the usual choice:

$$\phi = \frac{\tilde{\phi} D h_0}{IL\epsilon}, \quad \mathbf{u} = \frac{\tilde{\mathbf{u}} h_0^{d-1}}{QL}, \quad p = \frac{h_0^3 \tilde{p}}{\mu Q L \epsilon}, \tag{12}$$

where d is the space dimension, e.g., $d = 2,3$, and the pressure follows the viscous standard lubrication nondimensionalization.[22]

In the following, lower case letters refer to the inner region, while upper case ones refer to the outer region far from the aperture minimum. Using such nondimensionalization, the diffusion problem (1) becomes

$$(\partial_z^2 + \epsilon\partial_y^2 + \epsilon^2\partial_x^2)\phi = 0, \tag{13}$$

exhibiting different scaling behaviors in the directions x,y and z. Nondimensional Stokes equation (4) also scales as

$$\begin{aligned} &-\epsilon\partial_x p + (\partial_z^2 + \epsilon\partial_y^2 + \epsilon^2\partial_x^2)u = 0, \\ &-\sqrt{\epsilon}\partial_y p + (\partial_z^2 + \epsilon\partial_y^2 + \epsilon^2\partial_x^2)v = 0, \\ &-\partial_z p + (\partial_z^2 + \epsilon\partial_y^2 + \epsilon^2\partial_x^2)w = 0. \end{aligned} \tag{14}$$

III. TWO-DIMENSIONAL GEOMETRIES

A. Electrical problem

1. Inner expansion

The governing equation (13) has the standard feature of boundary layer equations that the potential must be constant at leading order across the inner region. This feature follows from the different scaling of its spatial variations on different directions. Thus we seek an expansion in small ϵ:

$$\phi = \phi_0 + \epsilon^2\phi_2 + O(\epsilon^3). \tag{15}$$

This choice derives from the realization that, in two dimensions, the governing equation for the $O(\epsilon)$ perturbation ϕ_1 is only a copy of the leading order. The boundary condition being also identical, this perturbation term must be equal to zero. Each perturbation then follows the governing equations:

$$\partial_z^2\phi_0 = 0, \tag{16}$$

with boundary condition

$$\partial_z\phi_0 = 0, \text{ on } z = 0 \text{ and } z = \hat{h}. \tag{17}$$

This problem is easily solved from stating a constant vertical potential gradient. The potential variation along the x direction is thus deduced by imposing a constant integrated flux along the vertical direction. In nondimensional form this simply writes $h(x)\partial_x\phi_0 = 1$, which can then be integrated, at leading order:

$$\phi_0(x) = \int_0^x \frac{dx}{1 + \frac{1}{2}x^2} = \sqrt{2}\arctan\left(\frac{x}{\sqrt{2}}\right). \tag{18}$$

The second order can thus be computed from this leading order using the governing equation:

$$\partial_z^2\phi_2 + \partial_x^2\phi_0 = 0. \tag{19}$$

The boundary condition at $O(\epsilon^2)$ order is given by expanding (2):

$$\begin{aligned} &\partial_z\phi_2 = 0 \quad \text{on } z = 0, \\ &-\tfrac{1}{2}\partial_z\phi_0 z^2 - x\partial_x\phi_0 + \partial_z\phi_2 = 0 \quad \text{on } z = \hat{h}. \end{aligned} \tag{20}$$

The solution can be computed up to a function of x only. This function can be found by imposing a zero flux associated with this second order potential:

$$\phi_2(x,z) = -\frac{1}{2}\frac{xz^2}{\hat{h}^2} - \frac{x}{2} + \frac{2\sqrt{2}}{3}\arctan\frac{x}{\sqrt{2}}. \tag{21}$$

2. Outer expansion

Similarly the length scale for variations in the vertical direction far from the constricted region is no longer the gap thickness but becomes the curvature h_{xx} of the aperture field. In this far-field region, horizontal variations are of the order of L, the distance between the aperture maxima. This requires rescaling

$$\begin{aligned} &(z,h) = \epsilon'^{-2}(Z,H), \\ &x = \epsilon^{-1}\epsilon'^{-1}X, \end{aligned} \tag{22}$$

where we introduce a new small parameter $\epsilon' = 1/(Lh_{xx})$ which is the typical slope of the aperture field. This rescaled

region can be considered to be the outer region of large inner variations, if the slope fulfills $\epsilon \ll \epsilon' < 1$. Using scaling (22), the governing equations become

$$\partial_Z^2 \Phi + \epsilon'^2 \partial_X^2 \Phi = 0. \tag{23}$$

It will be confirmed by examining the matching of boundary conditions coming from the inner region that the outer solution should be expanded as

$$\Phi = \Phi_0 + \frac{\epsilon}{\epsilon'} \Phi_1 . \tag{24}$$

The leading order outer potential must fulfill

$$\partial_Z^2 \Phi_0 = 0 \tag{25}$$

with boundary conditions

$$\partial_Z \Phi_0 = 0, \text{ on } Z = 0 \text{ and } Z = H. \tag{26}$$

The leading order outer solution is thus a constant, $\Phi_0(X,Z) = \Phi_0$, the value of which has to be matched with the inner region. The next order outer problem depends on the value of the ratio ϵ/ϵ'. Let us first consider the case $\epsilon/\epsilon' \gg \epsilon'^2$.

In this case, the first perturbation Φ_1 will fulfill the same problem and boundary conditions as the leading order. A general solution of this problem will be a function $\Phi_1(X)$ of X only. This function must verify the conservation of flux, integrated along the vertical direction, which imposes that $H\partial_X \Phi_1$ is a constant. Hence, it is defined up to an initial flux that has to be matched with the inner region. Hence, contrary to the leading order, there will be some supplementary flux coming out of the inner region associated with this corrective term.

In the case where $\epsilon/\epsilon' = \epsilon'^2$, the problem looks somewhat different for the first perturbation. It is precisely similar with the previously first perturbation problem in the inner (21):

$$\partial_Z^2 \Phi_1 + \partial_X^2 \Phi_0 = 0. \tag{27}$$

The boundary condition is given by expanding (2):

$$\begin{aligned} &\partial_Z \Phi_1 = 0 \quad \text{on } Z = 0, \\ &-\tfrac{1}{2} \partial_Z \Phi_0 Z^2 - X \partial_X \Phi_0 + \partial_Z \Phi_1 = 0 \text{ on } Z = H, \end{aligned} \tag{28}$$

Nevertheless, the leading order being constant, this problem degenerates, and we can recognize the previously examined problem for the leading order. We thus reach the same conclusion that $H\partial_X \Phi_1$ is a constant that has to be matched with the inner region.

3. Matching

We match the inner and outer solutions with the intermediate variable method, the result of which gives

$$\begin{aligned} &\Phi_0 = \phi_0(\infty) = -\frac{\sqrt{2}\pi}{2}, \quad \Phi_1(0) = 0, \\ &\partial_X \Phi_1(0) = \partial_x \phi_2(\infty) = -\tfrac{1}{2}. \end{aligned} \tag{29}$$

A symmetrical result holds when matching the first maximum region with the inner in the limit $x \to -\infty$. From this solution, we deduce a simple expression for the first correction to the outer, $H\partial_X \Phi_1 = -\frac{1}{2} H(0)$, which, from (22) and (9), leads to

$$\begin{aligned} \Phi_1(X_2) - \Phi_1(X_1) &= -\frac{1}{2} \int_{X_1}^{X_2} \frac{\epsilon^2 dX}{H(X)} \\ &= -\frac{1}{2} \epsilon\epsilon' \int_{X_1/\epsilon\epsilon'}^{X_2/\epsilon\epsilon'} \frac{dx}{h(x)} \\ &= -\frac{\pi}{2} \epsilon\epsilon' + O(\epsilon^2\epsilon', \epsilon^2\epsilon'^2). \end{aligned} \tag{30}$$

From (30) and (24) one can infer the asymptotic expansion for the potential drop between the two maxima,

$$\Delta\Phi = -\sqrt{2}\pi - \frac{\pi}{2}\epsilon^2. \tag{31}$$

This finally leads to the asymptotic expansion of the electrical conductance,

$$G = \frac{1}{\sqrt{2}\pi} \frac{h_0}{\epsilon} \left(1 - \frac{\epsilon^2}{2\sqrt{2}} \right), \tag{32}$$

which is the main result of this section. It is interesting to note that the $O(\epsilon^2)$ correction has an intrinsic algebraic form. In particular, there is no geometrical contribution coming from the conductance higher curvatures in the inner region. It will not be the case for permeability, as will be seen in the next section.

B. Stokes problem

1. Inner expansion

Following similar lines, the inner problem for Stokes pressure and flow-fields is expanded:

$$\begin{aligned} &p = \epsilon^{-1} p_0 + p_1 + \epsilon p_2, \\ &(u,w) = (u_0, \epsilon w_0) + \epsilon (u_1, \epsilon w_1) + \epsilon^2 (u_2, \epsilon w_2). \end{aligned} \tag{33}$$

The rescaling for the velocity field gives a self-consistent divergence-free flow field at each order. As in the diffusion problem, governing equations (14) give the same problem for the leading order and first perturbation $i = 0,1$:

$$\begin{aligned} &-\partial_x p_i + \partial_z^2 u_i = 0, \\ &-\partial_z p_i = 0, \end{aligned} \tag{34}$$

while the second order governing equations reads

$$\begin{aligned} &-\partial_x p_2 + \partial_z^2 u_2 + \partial_x^2 u_0 = 0, \\ &-\partial_z p_2 + \partial_z^2 w_0 = 0. \end{aligned} \tag{35}$$

This expansion has to be completed with consistent boundary conditions. In keeping with notation $\hat{h} = 1 + \frac{1}{2}x^2$, boundary conditions (6) are expanded,

$$u_0(x,\hat{h})=0,$$

$$u_1(x,\hat{h})=-\gamma_3\frac{x^3}{\hat{h}}\partial_z u_0(x,\hat{h}), \tag{36}$$

$$u_2(x,\hat{h})=-\gamma_4\frac{x^4}{\hat{h}}\partial_z u_0(x,\hat{h})-\frac{1}{2}\gamma_3^2\frac{x^6}{\hat{h}^2}\partial_z^2 u_0(x,\hat{h}) - \gamma_3\frac{x^3}{\hat{h}}\partial_z u_1(x,\hat{h}),$$

so that each order can be deduced from the previous one. Hence, in the case of the Stokes problem, the first perturbation is not a copy of the leading order because it fulfills different boundary conditions. At leading order, the Reynolds approximation is found again,

$$u_0(x,z)=\tfrac{1}{2}\partial_x p_0(x) z(z-\hat{h}). \tag{37}$$

The resulting flux being unity in this nondimensional formulation, the pressure is thus obtained from integrating the pressure gradient coming from the Darcy-type pressure-flux relation $\partial_x p_0(x)=-12/\hat{h}^3$:

$$p_0(x)=-\frac{3}{\hat{h}^2}-\frac{9x}{2\hat{h}}-\frac{9\sqrt{2}}{2}\arctan\frac{x}{\sqrt{2}}, \tag{38}$$

where the pressure reference is chosen as equal to zero at $x=0$. The next order solution for the velocity field is as simple as the leading order, to solve a boundary layer problem with uniform pressure along the vertical direction:

$$u_1(x,z)=\frac{1}{2}\partial_x p_1(x) z(z-\hat{h})-\frac{1}{2}\frac{zx^3}{\hat{h}}\gamma_3\partial_x p_0(x). \tag{39}$$

The first perturbation pressure gradient is then easy to get from imposing a zero flux on the first velocity perturbation. The integration of this pressure gradient gives

$$p_1(x)=-6\gamma_3\left(-\frac{3}{\hat{h}^4}+\frac{4}{\hat{h}^3}\right). \tag{40}$$

In principle, solving the next order problem (35) requires the solution for the vertical component of the velocity at leading order. Even though it is easy to compute, computation is not necessary; instead one can use incompressibility in order to find a relation between the velocity components derivative in each direction. This leads to a simple decomposition of the second order pressure $p_2(x,z)$, which depends on the vertical direction, as $p_2(x,z)=\partial_x u_0(x,z)+\hat{p}_2(x)$ with a yet unknown boundary layer additional contribution $\hat{p}_2(x)$. From this decomposition we solve the first momentum equation of (35) and find the formal solution for the velocity field second order perturbation:

$$u_2(x,z)=\frac{1}{2}\partial_x\hat{p}_2 z(z-\hat{h})-\frac{x^3 z\gamma_3}{2\hat{h}}\partial_x p_1-\frac{z}{2\hat{h}}\partial_x p_0\gamma_4 x^4 - \frac{1}{12}\partial_x^3 p_0 z(z-\hat{h})(z^2-\hat{h}z-\hat{h}^2). \tag{41}$$

Imposing a zero flux from this second order perturbation leads to defining the second perturbation boundary layer pressure gradient as

$$\partial_x\hat{p}_2=-\frac{1}{5}\hat{h}^2\partial_x^3 p_0-\frac{1}{2}\partial_x p_0\left(\frac{6x^4\gamma_4\hat{h}^2-18x^6\gamma_3^2}{\hat{h}^4}\right). \tag{42}$$

From this pressure gradient we found an expression for the second order perturbation pressure. As will be outlined in the next section, the matching will only require the asymptotic limit as $x\to\infty$ of this perturbed pressure. Integrating (42) with zero reference pressure at $x=0$ leads to

$$\lim_{x\to\infty} p_2=\lim_{x\to\infty}\hat{p}_2=\tfrac{9}{4}\pi\sqrt{2}\left(\tfrac{4}{5}+\tfrac{3}{4}\gamma_4-\tfrac{15}{16}\gamma_3^2\right). \tag{43}$$

2. Outer expansion and matching

Rescaling (22) is similarly applied in the outer domain for the Stokes problem. The governing equation (14) thus becomes

$$-\partial_X P+\left(\frac{\epsilon^3}{\epsilon'}\partial_Z^2+\epsilon^3\epsilon'\partial_X^2\right)U=0,$$
$$-\partial_Z P+(\epsilon^2\partial_Z^2+(\epsilon\epsilon')^2\partial_X^2)W=0. \tag{44}$$

The first perturbation of the outer problem must then be expanded in the following form:

$$P=P_0+\frac{\epsilon^3}{\epsilon'}P_1,$$
$$(U,W)=(U_0,\epsilon' W_0)+\frac{\epsilon^3}{\epsilon'}(U_1,\epsilon' W_1). \tag{45}$$

Being interested in an $O(\epsilon^2)$ correction, we will restrict our attention to the leading order of the outer perturbation, as usual for lubrication problems,[22] while, moreover, since here $\epsilon/\epsilon'\ll 1$, it is not necessary to compute the next order.

The matching for the far-right outer region then gives the following outer pressure:

$$P_0(X_2)=p_0(\infty)+\epsilon^2 p_2(\infty) = \tfrac{9}{4}\pi\sqrt{2}(1+\epsilon^2(\tfrac{4}{5}+\tfrac{3}{4}\gamma_4-\tfrac{15}{16}\gamma_3^2)). \tag{46}$$

A symmetrical result holds for matching the left outer region in the limit $x\to-\infty$, so that the hydraulic conductance can finally be computed:

$$K=\frac{\sqrt{2}}{9\pi}\frac{h_0^3}{\epsilon}\left(1-\epsilon^2\left(\frac{4}{5}+\frac{3}{4}\gamma_4-\frac{15}{16}\gamma_3^2\right)\right), \tag{47}$$

where we recall that $\gamma_3=h_{\tilde{x}\tilde{x}\tilde{x}}/(6h_{\tilde{x}\tilde{x}}^2)$ and $\gamma_4=h_{\tilde{x}\tilde{x}\tilde{x}\tilde{x}}/(24h_{\tilde{x}\tilde{x}}^3)$. The leading order exhibits the well-known[10,14,15] small gap dependence on $h_0^{5/2}$. The $O(\epsilon^2)$ correction has an intrinsic dependence on the third and fourth derivative at the gap minimum. It is worthwhile comparing this result with other lubrication results associated with moving particles. When considering the resistance matrix associated with the relation between forces and velocities it is well known that cubic and quartic terms do not generally contribute to the same correction order.[29–32] This is not the case

here, where both third and quartic derivatives fulfill a quadratic ϵ correction. Moreover, one can see that, depending on the sign of the quartic derivative, the correction could either increase or decrease the hydraulic conductance. Unsurprisingly, positive quartic derivative associated with profiles that are flatter than cylinders will decrease the hydraulic conductance. More surprisingly, any third derivative associated with an asymmetrical profile will lead to a hydraulic conductance increase.

These asymptotic results are interesting to compare with some approximate results obtained from saddle point approximations as studied by Borcea and Papanicolaou.[20,21] The Appendix shows that in two dimensions the saddle point approximation can be a rather precise estimate for the leading order.

IV. THREE-DIMENSIONAL GEOMETRIES

In the case of three-dimensional geometries we are interested in throat-like geometries [see Fig. 1(b)] resulting from the contact between a concave and a convex solid surface. The horizontal plane coordinate systems (x,y) associated with the principal direction at the saddle point are considered. They coincide with the Hessian eigenvectors directions at the saddle point. In this section we will focus on the leading order of the asymptotic expansion of conductances.

A. Asymptotic scaling

1. Diffusion problem

In three dimensions, the potential expansion must be taken in its general form:

$$\phi = \phi_0 + \epsilon\phi_1 + \cdots . \tag{48}$$

From now on, we will center on the first two perturbative terms. There should be an additional term of the order $O(\epsilon^{3/2})$ before the previously examined $O(\epsilon^2)$ because of the scaling of additional perturbation on the nondimensional aperture (11). Here we are following the same steps as in Sec. III A seeking the leading order potential ϕ_0 first. Expanding (48) in (13) leads to the same governing equation (16) and boundary conditions (17). Formally, the solution is the same and leads to a uniform potential over the vertical boundary layer, as well as along the transverse direction. This longitudinally varying potential gradient $\partial_x\phi_0(x)$ can thus be deduced from the imposed flux. Nevertheless, in three dimensions the flux should now be integrated over the vertical and the transverse directions. Expanding the aperture half-width y_0 from (11) leads to

$$y_0 = \sqrt{\frac{2\hat{h}}{-\epsilon\gamma_2}}\left(1 + \epsilon\frac{\gamma_3 x^3}{2\hat{h}} + O(\epsilon^{3/2})\right). \tag{49}$$

From nondimensionalization (12), integrating the potential gradient along z and y direction at leading order with a constant current intensity leads to

$$\begin{aligned}\epsilon^{-1/2} &= \int_{-y_0}^{y_0} dy \int_0^h dz\, \partial_x\phi_0(x) \\ &= \frac{4\sqrt{2}}{3}\sqrt{-\epsilon\gamma_2}\hat{h}^{3/2}\partial_x\phi_0(x),\end{aligned} \tag{50}$$

from which the potential solution at leading order can be integrated:

$$\phi_0(x) = \frac{3}{4\sqrt{-2\gamma_2\epsilon}}\frac{x}{\hat{h}^{1/2}}. \tag{51}$$

It is interesting to note that the leading order potential is not of order one, but it rather scales as $O(1/\epsilon)$ from the chosen nondimensionalization. This means that the three-dimensional diffusion conductance will scale linearly with h_0. As a matter of fact, the matching with the outer region, at leading order, will be as simple as adjusting the outer region's potential values to the limit of the inner potential (51) as x goes to infinity. It is then easy to find the asymptotic leading order for the three-dimensional electrical conductance:

$$G = \frac{2}{3}h_0\sqrt{\frac{h_{xx}}{-h_{yy}}}. \tag{52}$$

This result is very similar to the one obtained in Refs. 19 and 20 with a combination of reciprocity and extremal principle considerations. It is possible to compute the next perturbation order. One has first to realize that there will be $O(\epsilon)$ correction to the flux coming from the leading order, due to some geometrical contribution of (49) from integrating over small $O(\epsilon)$ correction to the gap width. This $O(\epsilon)$ contribution to the flux necessitates a nonzero first order correction to the potential in order to annihilate this flux correction. Using the same boundary conditions as the leading order one can compute the first order correction to the potential which is now not zero in three dimensions. It turns out that this correction is still localized inside the inner region, and does not bring any further contribution to the outer potential. The next possible correction should then be of order $O(\epsilon^{3/2})$.

2. Stokes problem

In three dimensions the pressure and velocity field have now to be expanded in the same way as in Sec. III B:

$$\begin{aligned}&p = \epsilon^{-1}p_0 + p_1, \\ &(u,v,w) = (u_0, \sqrt{\epsilon}v_0, \epsilon w_0) + \epsilon(u_1, \sqrt{\epsilon}v_1, \epsilon w_1).\end{aligned} \tag{53}$$

The leading order still corresponds to a boundary layer problem, for which the pressure is uniform over the vertical and transverse directions. The longitudinal velocity field u_0 can then be obtained from the first momentum equation of (34), so as to find the lubrication parabolic profile (37) again. This result can then be integrated to find the relation between the uniform imposed flux and the leading order pressure gradient $\partial_x p_0(x)$:

$$\epsilon^{-1/2} = \int_{-y_0}^{y_0} dy \int_0^h dz z(z-h)\partial_x p_0(x)$$

$$= \frac{16}{105\sqrt{2}} \sqrt{\epsilon\gamma_2}\hat{h}^{7/2}\partial_x p_0(x). \quad (54)$$

The longitudinally varying pressure p_0 can then be integrated from taking the reference pressure equal to zero at $x=0$:

$$p_0(x) = \frac{7}{8\sqrt{2}} \frac{1}{\sqrt{-\gamma_2\epsilon}} \frac{x(2x^4+10x^2+15)}{\hat{h}^{5/2}}. \quad (55)$$

Here again the leading order pressure is scaling as ϵ^{-1} due to nondimensionalization (12). This means from examining previous results (47) that the three-dimensional conductance will scale as h_0^3, as expected. As previously examined in Sec. III B 2, the matching of the pressure inner region with the outer pressure has in common with lubrication problems that the outer pressure leading order does not show any spatial variation. The outer pressure value is simply given by the $x \to \infty$ limit of the inner pressure. From (55) the leading order for the asymptotic hydraulic conductance thus reads

$$K = \frac{1}{14} h_0^3 \sqrt{\frac{h_{xx}}{-h_{yy}}}. \quad (56)$$

This leading order asymptotic estimate should give a good approximation of the pressure drop from imposing the flux in Fig. 1(b) throat. As was done previously, it is possible to compute further corrections. We focus on the first $O(\epsilon)$ terms, which still fulfill a simple boundary layer problem, as the leading order longitudinal velocity u_0 only shows a small $O(\epsilon)$ span-wise variation. Furthermore, as in the previous section, the leading order hydraulic flux has a small $O(\epsilon)$ contribution due to the integral over small $O(\epsilon)$ geometrical variations of the gap width. It is thus easy to find the inner pressure correction resulting from imposing a zero $O(\epsilon)$ flux. As for the diffusion problem, this pressure remains localized inside the inner region and does not bring any contribution to the outer pressure. The expected further contributions are of $O(\epsilon^{3/2})$ and $O(\epsilon^2)$.

The next section will present a numerical comparison between asymptotic results (52) and (56) with direct numerical computation.

B. Numerical computations

There are very few known exact results for the pressure in three-dimensional geometries and none of them can be used to test the validity of the proposed expression. Hence, numerical computation is necessary to check their accuracy and validity range. It is interesting to proceed from a simple aperture field to more complex ones. Hence, we first investigate a simple sinusoidal aperture field defined by

$$h'(X,Y) = \varepsilon + \frac{1}{\sqrt{2}}\left[-\frac{1}{\gamma_2}\cos(X) - \cos(Y) - \left(1+\frac{1}{\gamma_2}\right)\right],$$
$$h(X,Y) = H(h'(X,Y))h'(X,Y), \quad (57)$$

where H is the Heaviside function which imposes zero aperture at wherever the solid surfaces are in contact. The saddle point located at (0, 0) has an aperture equal to ϵ, with an associated Hessian eigenvalue ratio $\gamma_2 = h_{yy}/h_{xx}$. Hence, this sinusoidal aperture geometry has two free parameters ϵ and γ_2 for comparison with the proposed scaling. It is nevertheless worthwhile extending these tests to more general geometries. Hence we also have investigated randomly generated smooth aperture fields. This study is interested in short range correlated aperture fields with smooth derivative defined everywhere. For this Markovian family of random fields, a Gaussian short range correlation function has been chosen, the Fourier transform of which has a Gaussian power spectrum. From imposing such power spectrum on randomly generated aperture field in Fourier space one can back-transform them to generate aperture fields with prescribed correlation functions. Restricting our investigation to isotropic Gaussian correlation functions, several random fields have been generated with a high spectral accuracy (i.e., 256×256 points). In the following, two examples will be considered. The first is a closely isotropic aperture field associated with a Hessian eigenvalue ratio at the considered saddle point very close to one while the second is highly deformed in the y direction with $\gamma_2 \approx -2.59$ as represented in Fig. 1(b).

Numerical computation is performed with a standard finite volume technique on a Cartesian grid with a uniform grid spacing Δ in both (x,y) directions. The aperture field being periodic, (x,y) coordinates are rescaled between $[0,2\pi]$. Instead of solving full three-dimensional problems, we have rather chosen to investigate the aforementioned small-slopes limit where either the diffusion problem or the Stokes problem still does not exhibit potential or pressure variations. As already mentioned in earlier sections, these boundary layer problems can be formally solved concerning their vertical variations, while the in-plane potential or pressure will fulfill a heterogeneous Poisson problem:

$$\nabla\cdot(h(X,Y)\nabla\Phi) = 0,$$
$$\nabla\cdot(h^3(X,Y)\nabla P) = 0. \quad (58)$$

Both equations (58) have been solved with associated uniform Dirichlet boundary conditions $(\Phi,P)=0$ at $y=0$ and $(\Phi,P)=1$ at $y=2\pi$. The nodes associated with zero aperture are obviously disregarded by the solving procedure. The numerical solver uses a direct solving method. The influence of discretization is first investigated to quantify the validity range of the numerical results. Figure 2(a) illustrates the grid mesh influence when computing the hydraulic conductance for isotropic ($\gamma_2=-1$) sinusoidal aperture (57). As expected, the numerical computation diverges from the asymptotic limit as ϵ gets smaller. We thus define a critical ϵ_c associated with a given grid size $N\times N$ as the value of ϵ for which the relative error $|K-K_{512}|/K_{512}$ becomes greater than 10%. Better numerical results would have been obtained if more refined numerical methods[33] had been used. Figure 2(b) displays the ϵ_c variations with the discretization N. As

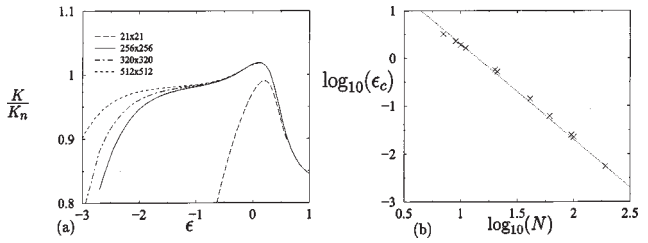

FIG. 2. (a) Evolution of ratio between the theoretical hydraulic conductance and its numerical computation K/K_n for four different grid sizes $N\times N$. (b) Critical gap ϵ_c versus the number of grid points N. The dashed line has a slope equal to -2.

can be seen, $\epsilon_c \propto N^{-2}$, i.e., $\epsilon_c \propto \Delta^2$, as expected from the chosen discretization method. Misorientation may have a considerable effect on numerical results with finite volume methods. These effects should be taken into account when saddle point principal directions are different from the mesh orientation. All these results indicate that any direct computation of conductances associated with a complicated aperture field with an increasing number of saddle points would rapidly become difficult, if not impossible, owing to the discretization level which is necessary for accurate results.

Figure 3(a) compares the numerical computation of the hydraulic conductance (for a grid mesh size $N=512$) to its asymptotic approximation. Three different geometries are represented, corresponding to the isotropic case ($\gamma_2=-1$) of Eq. (57) and the previously introduced randomly generated short-range correlated aperture fields. It is first interesting to note that for small values of ϵ, the hydraulic conductance reaches the asymptotic behavior (56), up to the expected numerical drift. One can observe that the difference between the predicted prefactor and the numerical results is smaller than 0.5%.

It is interesting to note the similarities in behavior between the sinusoidal aperture and the isotropic short-range correlated aperture for ϵ values as large as 10. While the anisotropic short-range correlated aperture clearly differs from the two other ones for ϵ values larger than 10^{-1}, it hardly differs from more than 30% for saddle point gap values as large as 10. This quantitative observation emphasizes the robustness of the leading order approximation (56). As a

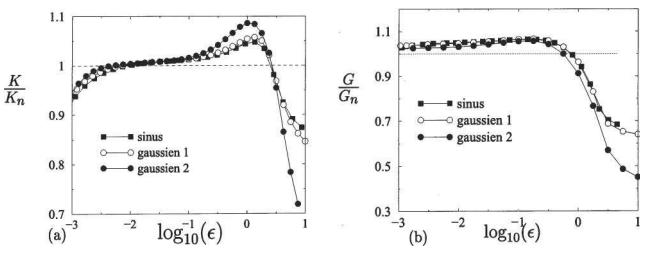

FIG. 3. Comparison between conductance K approximation (56) with numerical computations K_n. Square symbols are for sinusoidal aperture defined in (57) with $\gamma_2=-1$, while circle symbols are for random field short-range correlated apertures. Dark circles correspond to the aperture field represented on Fig. 1(b) with associated Hessian eigenvalue ratio equal to $\gamma_2=-2.59$, while opened circles are for an associated Hessian eigenvalue ratio equal to $\gamma_2=-1.05$. (b) Same convention as (a) for G.

matter of fact, the results displayed in Fig. 3(a) suggest that when the upper and lower surfaces have only few contact points (with associated saddle point gap close to one), the proposed approximation is approximately 10%. Moreover, the Hessian eigenvalue ratio appears as the main parameter accounting for deviations from the asymptotic leading order.

The numerical results sketched in Fig. 3(b) for the diffusive case qualitatively agree with those obtained for the hydraulic conductances. No numerical drift from the asymptotic behavior (52) is observed as ϵ gets smaller. This is due to the smoother behavior of the local conductance that is much easily captured by the numerical discretization. It could be clearly observed that the prefactor leading order is within 1% of numerical results. These numerical results are very similar to those obtained by Borcea and Papanicolaou[20] for which the comparison between numerical computation for the electrical resistance of a saddle point geometry was found to be very close to asymptotical results derived from extremal principle. Moreover, the results shown in Fig. 3(b) indicate that the asymptotic behavior (52) is also robust over quite a significant range of ϵ values.

These numerical results obtained from either deterministic analytical aperture fields or randomly generated ones show the fact that the proposed general conductances can provide a correct evaluation of any general saddle point geometry, as long as the surface slopes remain small.

V. CONCLUSION

Newtonian lubrication flow and diffusion transport through a constriction have been studied. Asymptotic expansion for electrical and hydraulic conductances has been obtained for two-dimensional (i.e., one-dimensional geometry) flow. Standard leading order results and the first asymptotic correction have been obtained. These results are simply expressed in terms of the minimum local geometry and do not depend on the far-field boundary conditions. Asymptotic expansion has also been used to study three-dimensional (i.e., two-dimensional lubricated flow) constrictions, the scaling of which has been obtained as a function of the saddle point eigenvalues ratio. The prefactors of the leading order have been analytically obtained and successfully compared with direct numerical computation. This leading order lubrication approximation has proved valid over a quite large range of constriction apertures. These results open up interesting perspectives to compute the flow through highly complicated geometries with a large number of constrictions.

The extension of the obtained results to low Mach number gas flows is a straightforward one. Because the conductances of compressible gas flows linearly vary with density, they will depend on the local pressure. As long as the no-slip boundary condition at the wall can be used (continuum flow), the dependence of the gas conductance on pressure is directly related to the gas state equation. Hence, even if the resulting pressure equation is nonlinear, one can easily find a suitable potential choice to linearize it. The resulting problem can then be matched with the one studied here, while

adapting the corresponding potential difference to the far-field pressure difference.

ACKNOWLEDGMENTS

The research presented in this article has been supported by GDR 2345 ''Etanchéité statique par joints métalliques en conditions extrêmes'' and encouraged by CNES, Snecma-Moteur, EDF and CNRS. Preliminary discussions with J. F. Luciani at the beginning of this work are gratefully acknowledged. So are enlightening discussions with Professor E. J. Hinch and H. Stone. We are especially indebted to H. Stone for finding the leading order asymptotic expression for the three-dimensional hydraulic conductance.

APPENDIX A: ASYMPTOTIC LEADING ORDER FOR TWO-DIMENSIONAL CONDUCTANCES

Integrating Eq. (17) for the electrical potential and (37) for the pressure leads to the closed form for leading order resistances computed from far field aperture maxima at positions X_1 and X_2,

$$\langle h^{-n}\rangle = \int_{X_1}^{X_2} h(x)^{-n}\,dx, \tag{A1}$$

with $n=1$ and $n=3$. For periodic aperture the conductance is integrated over a period, while for unbounded aperture $h(x)$ the integral domain is extended to infinity. Using expansion (11) in the vicinity of minimum $x=0$, and substituting this expansion in (A1), gives

$$\langle h^{-n}\rangle = \frac{h_0^{-n+1}}{\sqrt{\epsilon}} I_0^n + O(\epsilon)$$

in which coefficients I_0^n is given by $I_0^n = \int [1/(1+\frac{1}{2}x^2)^n]\,dx$. Carrying out the integrations leads to

$$\langle h^{-n}\rangle = \frac{h_0^{-n+1}}{\sqrt{\epsilon}} \frac{(n-1)!(n-2)!2^{2n-7/2}}{(2n-3)!\,\pi} + O(\epsilon). \tag{A2}$$

Obviously, these prefactors are exactly identical to those obtained from an exact integration of a simple sinusoidal profile:

$$h(x) = 1+\epsilon+\cos x.$$

For this type of aperture field, the integrations can be performed exactly.[14,15] Computation of the resistances yields

$$\langle h^{-n}\rangle = \int_0^{2\pi} \frac{1}{(1+\epsilon+\cos x)^n}\,dx = \frac{2\pi}{(1+\epsilon)^n} S(C,n) \tag{A3}$$

in which $S(C,n)$ is the Sommerfeld integral[34] defined by $S(C,n) = (1/2\pi)\int_0^{2\pi} dx/(1+C\cos x)^n$ with $C=1/(1+\epsilon)$. For $n=1,3$ it reads

$$S(C,1) = \frac{1}{\sqrt{1-C^2}}, \quad S(C,3) = \frac{2+C^2}{2(1-C^2)^{5/2}}.$$

From these exact results, one can derive asymptotic approximations as $\epsilon \ll 1$,

$$\langle h^{-1}\rangle = \frac{1}{\pi\sqrt{2}} h_0 \epsilon^{-1/2} + O(\epsilon),$$

$$\langle h^{-3}\rangle = \frac{4\sqrt{2}}{3\pi} h_0^3 \epsilon^{-1/2} + O(\epsilon),$$

which hopefully perfectly match the previous result (A2).

APPENDIX B: COMPARISON WITH GENERALIZED SADDLE POINT APPROXIMATION

In this appendix, we use the generalized saddle point approximation technique to obtain an estimate of the hydraulic conductance in two dimensions. Starting from Eq. (A1),

$$\langle h^{-n}\rangle = \int h(x)^{-n}\,dx, \tag{B1}$$

which is written as

$$\langle h^{-n}\rangle = \int \exp(-n\ln(h(x)))\,dx.$$

Changing variable x to $X=\sqrt{\epsilon}x/h_0$ leads to expressing the aperture field in the vicinity of the minima as

$$h(X) = h_0(1+\tfrac{1}{2}X^2),$$

while neglecting $O(\epsilon^{3/2})$ terms conductances can be written

$$\langle h^{-n}\rangle = C_n h_0^{-n+1/2} \frac{1}{\sqrt{h_{xx}}},$$

which, in agreement with the derivations presented in Sec. II, shows that, to the leading order in ϵ, the conductances depends on the seconds derivative of the aperture at the saddle point and on a numerical prefactor that is expressed in integral form as

$$C_n = \int \exp\left(-n\ln\left(1+\frac{1}{2}X^2\right)\right) dX. \tag{B2}$$

An approximation of the value of this prefactor can be obtained using a saddle-point approximation. Writing

$$g^2(X) = n\ln(1+\tfrac{1}{2}X^2),$$

the constant C_n defined in (B2) now becomes a Gaussian integral:

$$C_n = \int \exp(-g^2)\frac{1}{dg/dX}\,dg.$$

From expressing dX/dg in power series of g, $dX/dg = \Sigma_{m=0}^{\infty} a_m g^m$, one can tackle integration from Gaussian moments $\int e^{-g^2} g^{2m}\,dg = \sqrt{\pi}(2m-1)!!/2^m$. In the case $n=3$, one finds

$$\frac{dX}{dg} = \frac{\sqrt{6}}{3} + \frac{\sqrt{6}}{12}g^2 + \frac{25\sqrt{6}}{2592}g^4 + \cdots,$$

from which the leading order prefactor of the hydraulic conductance can be computed:

$$\langle h^{-3}\rangle = h_0^{-5/2}\frac{1}{\sqrt{h_{xx}}}\sqrt{\frac{2\pi}{3}}\left(1+\frac{1}{8}-\frac{225}{10\,268}\right).$$

Numerically, the successive order $m=0,2,4$ gives 1.44, 1.628, 1.661, which can be compared with the exact result $3\pi/4\sqrt{2}$, leading respectively to 10%, 1.6% and 0.3% estimate.

[1] R. Zimmerman and G. Bodvarsson, "Hydraulic conductivity of rock fractures," Trans. Por. Med. **23(1)**, 1 (1996).
[2] P. Adler and J. Thovert, *Fractures and Fracture Networks* (Kluwer Academic, Amsterdam, 1999).
[3] H. Butcher, "Fundamental principles for static sealing with metal in high pressure field," ASME Trans. **16**, 304 (1973).
[4] S. Matthias and F. Müller, "Asymmetric pores in a silicon membrane acting as massively parallel Brownian ratchets," Nature (London) **424**, 53 (2003).
[5] H. M. Martin, "The lubrication of gear teath," Engineer (London) **102**, 119 (1916).
[6] J. B. Keller, "Viscous flow through a grating or lattice cylinders," J. Fluid Mech. **18**, 94 (1964).
[7] M. J. Manton, "Low Reynolds number flow in slowly varying axisymmetric tubes," J. Fluid Mech. **49**, 451 (1971).
[8] S. Sisavath, X. Jing, and R. W. Zimmerman, "Creeping flow through a pipe of varying radius," Phys. Fluids **13**, 2762 (2001).
[9] J. Happel and H. Brenner, *Low Reynolds Number Hydrodynamics* (Kluwer, Amsterdam, 1983).
[10] S. Richardson, "A model for the boundary condition of porous material p2," J. Fluid Mech. **49**, 327 (1971).
[11] G. I. Taylor, "A model for the boundary condition of porous material p1," J. Fluid Mech. **49**, 319 (1971).
[12] M. Hemmat and A. Borhan, "Creeping flow through sinusoidally constricted capillaries," Phys. Fluids **7**, 2111 (1995).
[13] P. K. Kitanidis and B. B. Dykaar, "Stokes flow in a slowly varying two-dimensional periodic pore," Trans. Por. Med. **26**(1), 89 (1997).
[14] Y. Bernabe and J. F. Olson, "The hydraulic conductance of a capillary with a sinusoidally varying cross-section," Geophys. Res. Lett. **27**, 245 (2000).
[15] N. Letalleur, F. Plouraboué, and M. Prat, "Average flow model of rough surface lubrication: Flow factors for sinusoidal surfaces," ASME J. Tribol. **124**, 539 (2002).
[16] E. Hasegawa and H. Izuchi, "On steady flow through a channel consisting of an uneven wall and a plane wall," Bull. JSME **26**, 514 (1983).
[17] C. H. Wang, "Drag due to a striated boundary in slow Couette flow," Phys. Fluids **21**, 697 (1978).
[18] C. B. Shah and Y. C. Yortsos, "The permeability of strongly disordered systems," J. Fluid Mech. **8**, 280 (1989).
[19] S. M. Koslov, "Geometric aspects of averaging," Russ. Math. Surveys **44**, 91 (1989).
[20] L. Borcea and G. Papanicolaou, "Network approximation for transport properties of high contrast materials," SIAM (Soc. Ind. Appl. Math.) J. Appl. Math. **58**, 501 (1998).
[21] L. Borcea, "Asymptotic analysis of quasi-static transport in high contrast conductive media," SIAM (Soc. Ind. Appl. Math.) J. Appl. Math. **58**, 597 (1998).
[22] L. G. Leal, *Laminar Flow and Convective Transport Processes*, Butterworth–Heinemann Series in Chemical Engineering (Butterworth–Heinemann, Boston, 1992).
[23] H. A. Stone, "Pressure driven flow between and relative motion of corrugated or rough surfaces: Analytical results via higher order lubrication theory," Technical report, Harvard, DEAS, 1999.
[24] S. Kim and S. J. Karrila, *Micro-Hydrodynamics* (Butterworth-Heinemann, Boston, 1991).
[25] L. G. Leal, "Particle motion in a viscous liquid," Annu. Rev. Fluid Mech. **12**, 435 (1980).
[26] W. R. Dean and M. E. O'Neil, "A slow motion of viscous liquid caused by a rotation of a solid sphere," Mathematika **10**, 13 (1963).
[27] M. E. O'Neill and K. Stwartson, "On the slow motion of a sphere parallel to a nearby plane wall," J. Fluid Mech. **27**, 705 (1967).
[28] A. Goldman, R. G. Cox, and H. Brenner, "Slow viscous motion of a sphere parallel to a plane wall—I motion through a quiescent fluid," Chem. Eng. Sci. **22**, 637 (1967).
[29] P. Bungay and H. Brenner, "The motion of a closely fitting sphere in a fluid-filled tube," Int. J. Multiphase Flow **1**, 25 (1973).
[30] A. Falade and H. Brenner, "First-order wall curvature effects upon the Stokes resistance of a spherical particle moving in close proximity to a solid wall," J. Fluid Mech. **193**, 533 (1988).
[31] B. R. Hirschfeld, P. Bungay, and H. Brenner, "First and second order wall effects upon the slow viscous asymmetric motion of an arbirary shaped positioned and oriented particle within a circular cylinder," Physico-Chem. Hydrodyn. **5**, 99 (1984).
[32] R. G. Cox, "The motion of suspended particles almost in contact," Int. J. Multiphase Flow **1**, 343 (1974).
[33] L. Borcea and G. Papanicolaou, "A hybrid numerical method for high contrast conductivity problems," J. Comput. Appl. Math. **87**, 61 (1997).
[34] B. Hamrock, *Fundamentals of Fluid Film Lubrication* (McGraw–Hill, New York, 1994).